Dynamics and resilience of quantum correlations between two-mode Gaussian states in Gaussian environments

Y. Lahlou[a,*†], **M. Amazioug**[b,‡] , **B. Maroufi**[c,§] and **M. Daoud**[c,¶]

[a] *LPHE-MS, Department of Physics, Faculty of Sciences, Mohammed V University, Rabat, Morocco*

[b] *LPTHE, Department of Physics, Faculty of Sciences, Ibnou Zohr University, Agadir 80000, Morocco*

[c] *LPMS, Department of Physics, Faculty of Sciences, Ibn Tofail University, Kénitra, Morocco*

Abstract

Gaussian states, characterized by probability distributions in phase-space representations, play a fundamental role in quantum information processing. Despite their mathematical tractability, the presence of noise imposes limitations on achieving quantum protocols, impacting their effectiveness in continuous-variable quantum systems for various communication and computation tasks. Hence, investigating quantum entanglement and quantum correlations within the coherence of Gaussian states in noisy channels holds significant importance. In this study, we introduce and investigate a framework designed to precisely define and explore the dynamic evolution of quantum correlations within two-mode Gaussian states subjected to the effects of a Gaussian thermal environment. We elucidate the temporal progression of quantum correlations within an open system comprising two interconnected bosonic modes embedded in a Gaussian thermal environment. We explore the impact of the environment by considering the evolution of the initial parameters of the input states. We measure the quantum correlations by employing the quantifiers: the Gaussian logarithmic negativity (GLN) $\mathcal{N}$ and the Gaussian quantum discord (GQD) $\mathcal{D}_{\mathcal{G}}$. The behavior of these quantum correlation quantifiers is intricately related to the parameters of the input states utilized in the analysis. We demonstrate that the GQD $\mathcal{D}_{\mathcal{G}}$ serves as an appropriate measurement quantifier in capturing fundamental quantum correlations, outperforming other quantifiers. Furthermore, our findings reveal that the GQD $\mathcal{D}_{\mathcal{G}}$ exhibits greater resilience compared to GLN $\mathcal{N}$, showing a reduced sensitivity to external influences.

keywords: Gaussian states, quantum correlations, GLN, GQD, noisy Gaussian channels.
PACS: 03.67.-a, 03.65.-w, 03.65.Ta.

*Corresponding author.
†email: youness_lahlou@um5.ac.ma
‡email: m.amazioug@uiz.ac.ma
§email: mbouchra@hotmail.com
¶email: m_daoud@hotmail.com

1 Introduction

Quantum information [1, 2] seeks to handle and transmit data by leveraging the distinct aspects of quantum mechanics, wherein information bits are represented and encoded within quantum states. Recently, there has been a notable surge in advancing quantum information processing, driven by enhancements in quantum communication [3–5], quantum measurement [6–8], and quantum computing [9, 10]. Initially, the majority of quantum protocols were conceived for quantum-discrete variables (DV) [11], particularly quantum bits, employing physical systems like photons, ions, atoms, solid-state, superconducting devices, and nuclear magnetic resonance [12]. Also, there has been a growing emphasis on investigating continuous variable (CV) systems for executing quantum information processing tasks [1, 13, 14, 18]. To conduct various quantum information processes, implementing and manipulating continuous-variable (CV) systems in experimental settings is more straightforward compared to discrete quantum bits. Consequently, extensive research efforts have focused on CV systems from both theoretical and experimental perspectives.

Gaussian states, like squeezed coherent beams and twin beams [15], represent a specific subset of continuous variable (CV) systems that are manipulable in experimental settings [16, 17]. These states possess a distinctive formalism and serve as valuable tools for encoding and processing quantum information with continuous variables [18]. The degrees of freedom of Gaussian states are constrained solely to the displacement vector and the covariance matrix, contributing to their elegant mathematical formalism. Importantly, the Gaussian nature of these quantum states remains preserved through various quantum operations, whether unitary [19, 20] or non-unitary [21–24]. Gaussian states have succeeded in applications such as quantum teleportation and quantum error correction [25, 26]. Furthermore, their extensive use has been observed in manipulating quantum cloning, entanglement purification, and testing quantum non-locality [27, 28].

Undoubtedly, various quantum correlations[29], including quantum entanglement[30–33], non-locality [31, 34], serve as paramount elements in multiple quantum information processing fields, revolutionizing computational paradigms by enabling advanced manipulation and transmission of quantum information. Certainly, entanglement stands as an indispensable resource utilized across quantum computing [35], cryptographic protocols [36], and quantum teleportation [37], acknowledging its pivotal role in advancing these fields of quantum technology. Additionally, quantum entanglement has proven instrumental in enhancing detection within Gaussian quantum metrology [38–40], as well as refining quantum measurement strategies [41]. Recently, quantum entanglement, particularly in continuous variable (CV) systems such as Gaussian states, has emerged as a valuable asset in enhancing optical resolution [42–44], spectroscopy [45, 46], interferometry [47], tomography [48], and many other quantum operations [49].

Quantum information protocols require transmitting quantum correlations through non-unitary physical channels, making the execution of quantum processes challenging due to unavoidable environmental interaction in these channels. Consequently, quantum correlations deteriorate owing to

decoherence and dissipation caused by losses and noise [50]. Over recent decades, substantial efforts have been directed toward accurately describing quantum decoherence and the dynamics of quantum correlations within open quantum systems, notably in continuous variable (CV) systems. Within this realm, notable studies delve into the dynamics of quantum correlations in colored-noise environments [51, 53], system-reservoir interactions [54], the coupling of two qubits with bosonic baths [55], and the behavior of quantum correlations amidst decoherence [56, 57]. Along these lines of studies, our primary focus in this work is the detailed investigation of the dynamics of quantum correlations within noisy Gaussian channels.

This manuscript investigates quantum correlation dynamics in a quantum system involving two bosonic modes interacting with individual Gaussian thermal reservoirs. Each mode interacts distinctly with its thermal bath. The manuscript's structure includes Section 2, which introduces the essential aspects of Gaussian states as well as the Gaussian noise channels. Section 3 details the quantum correlation quantifiers adopted for analyzing the evolution of quantum correlations within our proposed protocol. Then, section 4 is concerned with the outcomes obtained from studying quantum correlation dynamics in channels affected by noisy environments, employing diverse quantum measures, specifically GQD and GLN. The paper ends with a final summary of the results.

2 The tools concepts of Gaussian state

Gaussian states constitute a foundational pillar in quantum mechanics, particularly in continuous variable systems. These kinds of quantum states, characterized by Gaussian probability distributions, play a pivotal role in quantum information processing due to their mathematical tractability and physical relevance. Exploring their properties unveils fundamental concepts crucial for comprehending quantum phenomena and their applications in various quantum protocols. Indeed, studying systems comprising bosonic modes entails comprehending their interactions, energy exchange, and time evolution within the framework of quantum mechanics. Such investigations hold immense significance across diverse domains including quantum optics [58], condensed matter physics [59], and quantum information processing, providing profound insights into fundamental quantum behavior and potential technological applications. Each bosonic mode is characterized by creation and annihilation operators, which depict particle creation and annihilation within each mode. To introduce the formalism of covariance matrix, we consider a system composed of m bosonic modes, where each mode $(k = 1, 2, ..., m)$ characterized by the set of the annihilation and creation operators $\hat{a}_k$ and $\hat{a}_k^\dagger$, following the commutation relations $[\hat{a}_k, \hat{a}_l^\dagger] = \delta_{kl}$. The system's Hilbert space $\mathcal{H}$ is the tensor product of infinite-dimensional Fock spaces $\mathcal{H} = \bigotimes_{k=1}^{m} \mathcal{F}_k$, with each $\mathcal{F}_k$ associated with mode k and spanning the number basis $\{|m\rangle_k\}_{k=1}^{m}$, comprising eigenstates of the number operator $\hat{a}_k^\dagger \hat{a}_k$. The Hamiltonian governing non-interacting modes is expressed as $H = \sum_{k=1}^{m} \left(\hat{a}_k^\dagger \hat{a}_k + \frac{1}{2}\right)$. The associated quadrature operators for the k^{th} mode, delineating

position, and conjugate momenta, are given by:

$$Q_k = \hat{a}_k^\dagger + \hat{a}_k, \qquad P_k = i\left(\hat{a}_k^\dagger - \hat{a}\right). \tag{1}$$

Here we set ($\hbar = 2$). The commutation relations between the quadrature operators are written as $[\hat{Q}_k, \hat{P}_l] = 2i\delta_{kl}$. These structure relations can be cast in compact form, using the blocks vector of quadratics operators $\hat{\mathbf{R}} = \left(\hat{Q}_1, \hat{P}_1, ..., \hat{Q}_m, \hat{P}_m,\right)^T$. This compact form allows us to express the commutation relations between these operators more concisely. Indeed, the commutation relation between the k^{th} and l^{th} modes are written as:

$$\left[\hat{R}_k, \hat{R}_l\right] = 2i\Omega_{kl}, \tag{2}$$

where Ω_{kl} denotes the elements constituting the $2m \times 2m$ symplectic matrix defined by

$$\Omega = \bigoplus_{k=1}^{m} \omega, \qquad \omega = \begin{bmatrix} 0 & 1 \\ -1 & 0 \end{bmatrix}. \tag{3}$$

In an $m-$modes bosonic system, the density operator symbolized as ρ, provides a comprehensive representation of the quantum state. This density operator finds an equivalent mathematical tool through quasi-probability distributions in phase space, notably the characteristic function or the Wigner function [48, 60]. These distributions offer a unique perspective, allowing the visualization of quantum states in terms of phase space representations, and facilitating analysis and experimental characterizations of the system's behavior. This representation is known as the Wigner representation [61]. In this context, the entire quantum information encoded within the density operator ρ is analogously encoded within the displacement vector $\boldsymbol{d} = \left\langle \hat{\boldsymbol{R}} \right\rangle$ and the covariance matrix defined within the phase space given by

$$\sigma_{kl} \equiv [\sigma]_{kl} = \frac{1}{2}\left\langle \hat{R}_k\hat{R}_l + \hat{R}_l\hat{R}_k \right\rangle - \left\langle \hat{R}_l \right\rangle \left\langle \hat{R}_k \right\rangle, \tag{4}$$

where $\left\langle \hat{O} \right\rangle = \mathrm{Tr}[\rho\hat{O}]$ represents the expectation value of the operator $\hat{O}$ in the quantum state described by the density matrix ρ. The covariance matrix σ is a $2m \times 2m$ real symmetric matrix, defined as positive definite, ensuring that all its eigenvalues are positive. This matrix σ satisfies the uncertainty relation as proposed by Simon in 1987 [62]

$$\sigma + i\Omega \geq 0. \tag{5}$$

This uncertainty relation provides insights into the inherent uncertainties associated with the measurements of pairs of observables in quantum systems, revealing fundamental limits on precision in certain quantum measurements. Importantly, the formalism of Gaussian states in quantum mechanics is extremely simple, since they are fully characterized by their first and second moments, which correspond to the mean values and variances of the quadrature operators. In general, a quantum state operation is represented by a map $\mathcal{E} : \rho \to \mathcal{E}(\rho)$, where ρ represents the initial state and $\mathcal{E}(\rho)$ represents the final state after operation. This map is required to be completely positive, meaning that it preserves the positivity of density matrices. In the context of quantum operations, two types of maps can be

distinguished. The first type is completely positive and trace-preserving, denoted as $\mathrm{Tr}\left[\mathcal{E}(\rho)\right] = 1$. This means that the map preserves the trace of the density matrix, which represents the probability conservation in quantum mechanics. The second type is a linear map that is completely positive and trace-decreasing, denoted as $\mathrm{Tr}\left[\mathcal{E}(\rho)\right] \leq 1$. In this case, the map can decrease the trace value of the density matrix. The first category of maps is associated with closed quantum channels that admit reversible transformations. These reversible maps can be described by unitary transformations $\hat{U}\hat{U}^{\dagger} = \mathbb{1}$, where $\mathbb{1}$ represents the identity operator, unitary transformations preserve both the normalization and purity of quantum states, which transform a quantum state according to

$$\hat{U} : \rho \to \hat{U}\rho\hat{U}^{\dagger}. \tag{6}$$

The unitary transformations that preserve the Gaussian characteristic of a given quantum state are known as Gaussian unitary channels. These channels are generated by the unitary evolution governed by hermitian Hamiltonian and expressed by $\hat{U} = \exp(-i\hat{H}t)$. The Hamiltonian takes the form of second-order polynomials in quadrature operators. Gaussian unitary transformations can be described in the phase space by symplectic transformations, which, in turn, are linear transformations that preserve the symplectic form

$$\hat{S}\Omega\hat{S}^{T} = \Omega, \tag{7}$$

where $\hat{S}$ is a $2m \times 2m$ real symplectic matrix that acts on the covariance matrix. In the phase space, the projection of the equation (6) gives

$$\hat{S} : \hat{\rho} \to \hat{S}\sigma\hat{S}^{T}. \tag{8}$$

In addition to the Gaussian unitary channels associated with the first type of maps $\mathcal{E} : \rho \to \mathcal{E}(\rho)$, the Gaussian non-unitary channels, also known as noisy Gaussian channels, play a crucial role in the implementation of quantum information processing [51]. These channels are characterized by noise and loss of quantum coherence due to interactions with the environment [51]. The study of these noisy Gaussian channels is important because they provide a realistic model for understanding and dealing with imperfections and noise in practical quantum systems [51, 52]. By considering these non-unitary transformations, researchers can develop strategies to mitigate or correct errors that may occur during quantum information processing tasks. Noisy Gaussian channels, also known as Gaussian non-unitary channels, are typically susceptible to noise and the loss of quantum coherence resulting from interactions with the environment. In this context, the dynamics of the m-mode bosonic system evolving under the influence of the noisy channel can be characterized by the following master equation:

$$\frac{\partial\rho}{\partial t} = \frac{\Gamma}{2}\left\{(N+1)\mathcal{L}[\hat{a}] + N\mathcal{L}\left[\hat{a}^{\dagger}\right] - M^{*}\mathcal{D}[\hat{a}] - M\mathcal{D}\left[\hat{a}^{\dagger}\right]\right\}\rho, \tag{9}$$

Here N denotes the mean thermal photon number of the environment (bath). The squeezing parameter of the bath, denoted by $M \in \mathbb{C}$, characterizes the degree of squeezing in the quantum state of the environment. It is a complex-valued parameter describing both the amount of squeezing $\left(|M| = \sqrt{M^{*}M}\right)$

and its direction $\left(\text{arctg}\frac{M}{\sqrt{M^*M}}\right)$. Additionally, Γ denotes the overall damping rate, describing how energy or information is lost from the system through dissipation and decoherence processes. The operators $\mathcal{L}[\hat{O}]\rho = 2\hat{O}\rho\hat{O}^\dagger - \hat{O}^\dagger\hat{O}\rho - \rho\hat{O}^\dagger\hat{O}$ and $\mathcal{D}[\hat{O}]\rho = 2\hat{O}\rho\hat{O} - \hat{O}\hat{O}\rho - \rho\hat{O}\hat{O}$ are the Lindblad super-operators, which describe open quantum systems and their evolution under dissipative processes. The terms proportional to $\mathcal{L}[\hat{a}]$ and $\mathcal{L}[\hat{a}^\dagger]$ represent losses and linear phase-insensitive amplification processes, respectively. On the other hand, the terms proportional to $\mathcal{D}[\hat{a}]$ and $\mathcal{D}[\hat{a}^\dagger]$ describe phase-dependent fluctuations. Physically, the Gaussian noisy channel describes the unavoidable interaction between the quantum system and its surrounding environment. In realistic optical implementations, such environmental coupling originates from photon losses, thermal fluctuations, imperfect transmission lines, and detector inefficiencies. These mechanisms induce decoherence and dissipation effects that progressively degrade the quantum properties of the propagated states. The parameter M describes the squeezing properties of the environment itself, allowing the bath to exhibit phase-sensitive fluctuations. Consequently, the considered Gaussian noisy channel provides a realistic framework for studying the robustness of quantum correlations under experimentally relevant conditions. The positivity of the density matrix imposes a constraint on the squeezing parameter and the effective number of photons, given by $|M|^2 \leq N(N+1)$. This condition guarantees the positivity of the density matrix, which is required for any physically admissible quantum state. When the system reaches thermal equilibrium, corresponding to the absence of squeezing ($M = 0$), the effective number of photons N coincides with the average number of thermal photons. In this regime, the system exhibits the characteristics of a thermal distribution.

Now, let us consider an m-mode input Gaussian state ρ_{inp} with second moments described by σ_{inp}. The non-unitary dissipative evolution preserves the Gaussian nature of the state. The time evolution of the second moments under dissipation is governed by the following equations of motion [63].

$$\frac{\partial \boldsymbol{\sigma}}{\partial t} = -\Gamma\left(\boldsymbol{\sigma} - \boldsymbol{\sigma}_\infty\right), \tag{10}$$

which leads to the following solution

$$\boldsymbol{\sigma}(t) = e^{-\Gamma t}\boldsymbol{\sigma}_{\text{inp}} + \left(1 - e^{-\Gamma t}\right)\boldsymbol{\sigma}_\infty, \tag{11}$$

in terms of asymptotic diffusion covariance matrix, denoted as $\sigma_\infty = \bigoplus_{k=1}^{m} \sigma_{k,\infty}$, that is associated with the effect imposed by the Gaussian environment. It represents the covariance matrix that emerges when the initial state is Gaussian and reaches a steady state under the influence of the environment. The specific form of σ_∞ can be determined solely in terms of the bath parameters such as

$$\boldsymbol{\sigma}_{k,\infty} = \frac{1}{2}\begin{pmatrix} \left(\frac{1}{2}+N\right) + \Re\text{e}[M] & \Im\text{m}[M] \\ \Im\text{m}[M] & \left(\frac{1}{2}+N\right) - \Re\text{e}[M] \end{pmatrix}. \tag{12}$$

The diffusion matrix represents the asymptotic covariance matrix when the initial state is Gaussian. In other words, it describes the spread and correlations of variables in a system that has reached a steady state under the influence of a Gaussian environment.

3 Quantum correlations quantifiers in Gaussian Systems

3.1 Gaussian Quantum Discord (GQD)

Gaussian quantum discord (GQD) [20, 64] is a measure of nonclassical correlations between subsystems A and B of a bipartite Gaussian state, denoted by ρ_{AB}. Unlike entanglement, GQD can capture quantum correlations that may exist even in separable states. Its evaluation involves the covariance matrix of the joint state and quantifies the quantum correlations that remain when local measurements are performed on one of the subsystems. It provides a broader perspective on quantum correlations relevant to quantum information processing and can be used to characterize the disturbance associated with local measurements. The properties of GQD have been investigated in various quantum systems, providing insights into quantum dynamics, phase transitions, and the resilience of quantum correlations in noisy environments, as well as their potential applications in quantum technologies. For two-mode Gaussian states, the covariance matrix is expressed as

$$\sigma_{AB} = \begin{pmatrix} \alpha & \gamma \\ \gamma^{\mathrm{T}} & \beta \end{pmatrix}, \tag{13}$$

where α and β are 2×2 covariance matrices for the single modes, and γ is a 2×2 covariance matrix containing cross-correlations between diverse modes. In this case, the Gaussian discord ($\mathcal{D}_{\mathcal{G}}$) in terms of the covariance matrix elements, takes the following form [20, 64]

$$\mathcal{D}_{\mathcal{G}} = f\left(\sqrt{\Upsilon}\right) - f\left(\tilde{\eta}_{+}\right) - f\left(\tilde{\eta}_{-}\right) + f\left(\delta\right) \tag{14}$$

where $f\left(x\right) = \left(x + \frac{1}{2}\right) \ln\left(x + \frac{1}{2}\right) - \left(x - \frac{1}{2}\right) \ln\left(x - \frac{1}{2}\right)$, and $\tilde{\eta}_{+}$ and $\tilde{\eta}_{-}$ are the symplectic eigenvalues given by

$$2\tilde{\eta}_{\pm}^{2} = \tilde{\Delta}(\sigma_{AB}) \pm \sqrt{\tilde{\Delta}(\sigma_{AB})^{2} - 4\mathrm{Det}\left(\sigma_{AB}\right)}, \tag{15}$$

with $\tilde{\Delta}(\sigma_{AB}) = \mathrm{Det}\alpha + \mathrm{Det}\beta - 2\mathrm{Det}\gamma$ in terms of the determinant of α, β, and γ that are components of the general covariance matrix Eq. (13). The quantity δ in (14) is given bay [65, 66]

$$\delta = \frac{\sqrt{\det \alpha} + 2\sqrt{\det \alpha \det \beta} + 2 \det \gamma}{1 + 2\sqrt{\det \beta}}. \tag{16}$$

3.2 Gaussian Logarithmic Negativity (GLN)

From a quantitative perspective, the GLN ($\mathcal{N}$) measures entanglement for general Gaussian states, capturing the quantum correlations between two subsystems and providing insights into the entanglement properties of quantum states. Initially introduced in Ref. [67] as an entanglement measure, GLN was further discussed and extended to continuous-variable (CV) systems in Refs. [65, 68]. This measure has proven particularly useful for studying the entanglement of Gaussian states in continuous-variable systems. It quantifies the amount of entanglement present in bipartite Gaussian states through the

negative eigenvalues arising from the partial transposition operation, thus providing valuable information about the entanglement structure. GLN can also be used to compare different Gaussian states or to monitor the evolution of entanglement dynamics over time. In summary, GLN ($\mathcal{N}$) is an entanglement measure specifically adapted to general Gaussian states. The GLN of a quantum state ρ is defined as

$$\mathcal{N}(\rho) = \frac{\|\rho^{T_B}\|_1 - 1}{2}, \tag{17}$$

where ρ^{T_B} is the partial transpose of the density matrix ρ with respect to the subsystem B, and $\|\cdot\|_1$ represents the trace norm.This measure quantifies the degree to which ρ^{T_B} deviates from being a positive matrix. A closely related entanglement quantifier is the *GLN* denoted as $\mathcal{N}$, defined by $\mathcal{N} \equiv \log\|\rho^{T_B}\|_1$. This GLN serves as an upper bound for the distillable entanglement of the quantum state ρ and is associated with the entanglement cost under Positive Partial Transpose (PPT) preserving operations, as discussed in [67]. The negativity as well as the GLN have been demonstrated to exhibit monotonic behavior when subjected to operations involving Local Operations and Classical Communications (LOCC). [65, 69, 70]. This property is essential for these measures to be considered valid entanglement quantifiers. Furthermore, the GLN exhibits the advantageous feature of additivity, confirming its utility in characterizing the entanglement properties of quantum states. For any bipartite Gaussian state represented by ρ, it can be readily demonstrated that both the negativity and the GLN exhibit straightforward monotonicity with respect to the parameter $\tilde{\eta}_-$ [65, 71].

$$|\rho^{T_B}|_1 = \frac{1}{\tilde{\eta}_-} \Rightarrow \mathcal{N}(\rho) = \max\left[0, \frac{1-\tilde{\eta}_-}{2\tilde{\eta}_-}\right] \tag{18}$$

$$\mathcal{N}(\rho) = \max\left[0, -\log\tilde{\eta}_-\right]. \tag{19}$$

These formulations explicitly measure the extent to which the essential and adequate Positive Partial Transpose (PPT) condition for separability is violated. The symplectic eigenvalue $\tilde{\eta}_-$ serves as a comprehensive and quantitative indicator, utilizing measures of negativities, to assess the entanglement present in a two-mode Gaussian state σ: if $\tilde{\eta}_- \geq 1$, the state is considered as separable; otherwise, it is classified as entangled. Notably, as the symplectic eigenvalue $\tilde{\eta}_-$ approaches zero, the negativities exhibit unbounded growth, signifying a profound increase in the entanglement content of the state.

4 Dynamics of GQD and GLN

In this section, we investigate the dynamics of quantum correlations in a two-mode bosonic system described by a Gaussian quantum state, in the presence of environmental interactions. To this end, we prepare an initial two-mode Gaussian state and study its evolution under a noisy Gaussian environment. Gaussian states are ubiquitous in continuous-variable quantum information because they are fully characterized by their first and second moments (the covariance matrix) and remain Gaussian under many relevant noise channels (e.g., thermal loss, amplification, dephasing). Here we focus on a bipartite

system consisting of two bosonic modes, A and B, initially prepared in a Gaussian state ρ_{AB} with covariance matrix σ_{AB}.

To probe the effect of noise on the system in an operational way, we introduce a local phase-encoding operation on mode A prior to the environmental interaction. This operation is implemented via the unitary transformation

$$\hat{U}_A^{\varphi}(\varphi) = \exp\left(i\varphi\hat{H}_A\right), \tag{20}$$

where φ is a real phase parameter and $\hat{H}_A$ is the corresponding generator acting on mode A. For simplicity, we assume that the spectrum of $\hat{H}_A$ is non-degenerate, which guarantees that distinct values of φ imprint distinguishable phase shifts. Typical choices for $\hat{H}_A$ include the number operator $\hat{n}_A = \hat{a}^\dagger\hat{a}$ (imprinting a phase on coherent states) or a quadrature operator such as $\hat{x}_A$ (generating displacements). The operation $\hat{U}_A^{\varphi}$ effectively encodes the parameter φ into the quantum state of mode A without affecting mode B.

The transformed bipartite state after phase encoding is given by

$$\rho_{AB}^{\varphi} = \left(\hat{U}_A^{\varphi}\otimes\mathbb{1}_B\right)\rho_{AB}\left(\hat{U}_A^{\varphi}\otimes\mathbb{1}_B\right)^\dagger. \tag{21}$$

We emphasize that the phase-encoding operation is not introduced as a full quantum metrology protocol, but rather as an operational tool to monitor how quantum correlations are affected by Gaussian noise. In a metrology setting one would typically optimize over measurements to estimate φ; here, instead, we use the encoding simply as a witness: the degradation of correlations under noise can be inferred by comparing how the phase-imprinted state evolves relative to the original one.

After the phase encoding, the system interacts with a Gaussian noisy environment. The environment is modelled as a Gaussian channel (e.g., a bosonic thermal channel or a phase-insensitive amplifier) that acts on both modes, possibly with memory effects if the channel is correlated. Because the initial state is Gaussian and the channel is Gaussian, the output state $\hat{\rho}_{\text{out}}$ remains Gaussian and is completely described by its covariance matrix σ_{out}. Although the main focus of this work is the dynamics of quantum correlations under Gaussian noise, the phase-imprinting operation provides a convenient framework to quantify how such correlations are degraded by environmental effects. For instance, by evaluating measures like GLN or GQD as functions of φ before and after the noise, one can extract the sensitivity of the correlations to the encoded phase and, hence, to the decoherence induced by the environment. A schematic representation of the protocol is shown in Fig. 1.

Within this study, the considered initial state is characterized by a combination of three fundamental Gaussian operations: squeezing, rotation, and displacement. Specifically, we consider a two-mode state generated from a separable two-mode thermal state by successively applying squeezing, rotation, and displacement transformations. The resulting state is parameterized by the squeezing factor r, the rotation angle θ, and the initial displacement vector $\boldsymbol{\alpha}$. This construction provides one of the most general representations of a two-mode Gaussian state. From a physical perspective, these Gaussian operations constitute essential tools in continuous-variable quantum optics experiments. The two-mode squeezing operation generates quantum correlations and entanglement between the bosonic modes

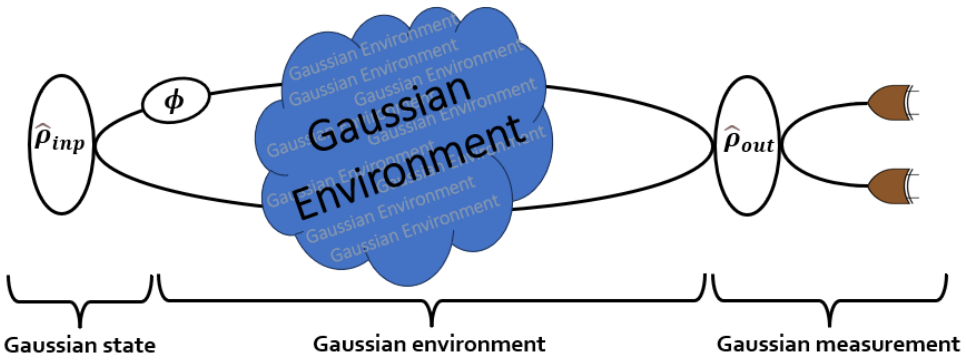


Figure 1: The figure outlines the three main stages: (i) preparation of the initial Gaussian state ρ_{AB}; (ii) local phase encoding on mode A; (iii) interaction with the Gaussian noisy environment, resulting in the output state $\hat{\rho}_{\text{out}}$. The subsequent analysis compares the quantum correlations in $\hat{\rho}_{\text{out}}$ with those in the encoded state before noise, revealing how environmental interactions erode the non-classical features of the system.

through correlated photon-pair creation processes, playing a crucial role in quantum communication and quantum metrology protocols by enhancing non-classical correlations and quantum sensitivity. The rotation operation corresponds to a phase-space rotation, or equivalently to the action of a beam splitter with tunable transmissivity, which redistributes correlations between the two modes while preserving the Gaussian nature of the state. Consequently, the rotation angle θ acts as a controllable parameter for manipulating the structure of quantum correlations. Furthermore, the displacement operation represents coherent excitation induced by external classical driving fields, shifting the Gaussian state in phase space without modifying its covariance properties. These Gaussian transformations are experimentally accessible using standard optical devices such as parametric amplifiers, beam splitters, and phase shifters, making the considered model physically relevant for continuous-variable quantum technologies. The density matrix describing this input state is expressed as follows

$$\hat{\rho}_{\text{inp}} = \hat{D}_2(\boldsymbol{\alpha})\hat{R}_2(\theta)\,\hat{S}_2(r)\,(\hat{\rho}_{th}\otimes\hat{\rho}_{th})\,\hat{S}_2(r)^{\dagger}\hat{R}_2(\theta)^{\dagger}\hat{D}_2(\boldsymbol{\alpha})^{\dagger}. \tag{22}$$

Here, the operator $\hat{S}_2(r)$ takes the form $\exp\left(r\left(\hat{a}_1^{\dagger}\hat{a}_2^{\dagger}-\hat{a}_1\hat{a}_2\right)\right)$, embodying the two-mode squeezing mechanism characterized by the squeezing parameter r. Additionally, the operator $\hat{R}_2(\theta) = \exp\left(\theta\left(a_1^{\dagger}a_2 - a_1a_2^{\dagger}\right)\right)$ is the two-mode rotational operator within the phase space, governed by the rotation angle θ. This operator finds correspondence with the Beamer splitter, featuring a transmissivity denoted by $\tau = \cos^2\theta$. The two-mode displacement operator, denoted as $\hat{D}_2(\boldsymbol{\alpha}) = \exp\left(\alpha_1\hat{a}_1^{\dagger} - \alpha_1^{*}\hat{a}_1 + \alpha_2\hat{a}_2^{\dagger} - \alpha_2^{*}\hat{a}_2\right)$ with the parameter vector $\boldsymbol{\alpha}$. In Equation (22), $\hat{\rho}_{th}$ represents the thermal state, which is

$$\hat{\rho}_{th} = \sum_{n_i}\frac{\bar{n}_i^{n_i}}{(\bar{n}_i+1)^{n_i+1}}|n_i\rangle\langle n_i|, \tag{23}$$

where $\bar{n}_i (i=1,2)$ denotes the mean photon number of the initial thermal state of the i-th mode of the system, determined by taking the trace of the multiplication $\text{Tr}\left(\hat{\rho}_{\text{th}}\hat{a}_i^{\dagger}\hat{a}_i\right)$. This average photon count's

reliance on temperature is captured by the formula $\bar{n}_i = \frac{1}{e^{\beta}-1}$, with β the inverse of the temperature. As the temperature nears absolute zero, the behavior of the thermal state for two modes tends toward the two-mode pure vacuum state, indicating a direct correlation between temperature and the quantum state's characteristics. Using equation (22), it can be verified that the corresponding Wigner function or characteristic function takes the Gaussian form, as described by a covariance matrix

$$\sigma_{\text{inp}} = \hat{R}_2(\theta)\hat{S}_2(r)\,(2\bar{n}_1+1)\,\mathbb{1}_{2\times 2} \oplus (2\bar{n}_2+1)\,\mathbb{1}_{2\times 2}\hat{S}_2(r)^{\dagger}\hat{R}_2(\theta)^{\dagger}. \tag{24}$$

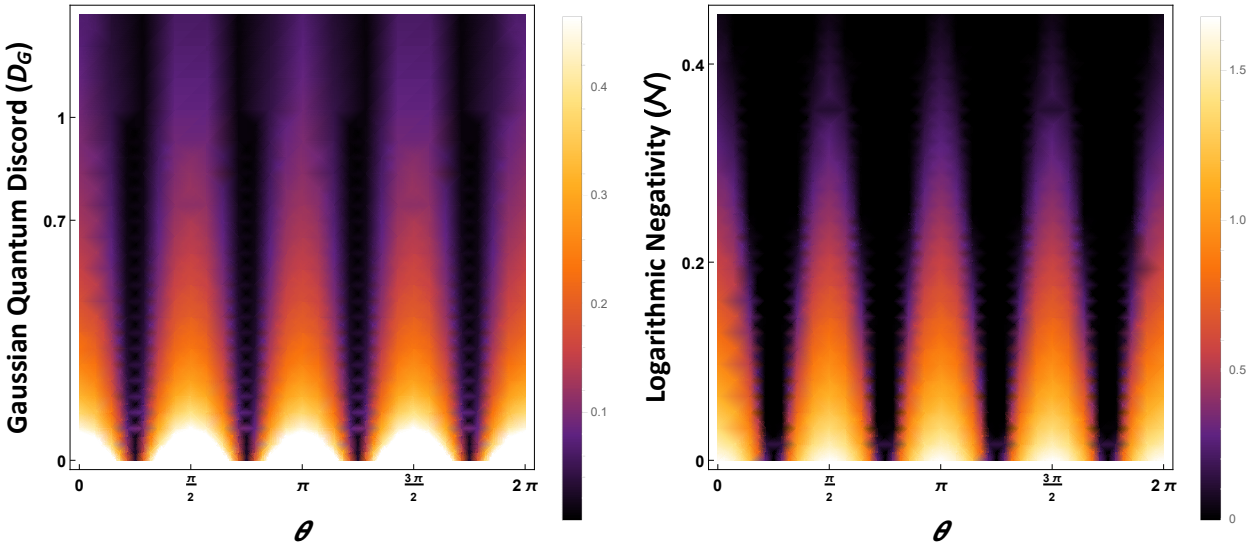
where $\hat{R}_2(\theta)$ and $\hat{S}_2(r)$ represent the symplectic transformations linked to rotation and squeezing operations, respectively. The progression of the two-mode bosonic system occurs through a non-unitary channel characterized by Gaussian noise, as outlined by the master equation (9). The evolution's depiction in the Wigner representation is articulated through the covariance matrix

$$\sigma_{\text{out}}(t) = e^{-\Gamma t}\left(U_A^{\varphi} \oplus \mathbb{1}_B\right)\sigma_{\text{inp}}\left(U_A^{\varphi} \oplus \mathbb{1}_B\right)^{\dagger} + \left(1-e^{-\Gamma t}\right)\sigma_{\infty}. \tag{25}$$

Regarding the Gaussian nature of the environment, it is noteworthy that as the squeezing parameter of the surroundings tends toward zero, the diffusion matrix σ_{∞} adopts a diagonal form. This writes

$$\sigma_{\infty} = (2\bar{n}_1+1)\,\mathbb{1}_{2\times 2} \oplus (2\bar{n}_2+1)\,\mathbb{1}_{2\times 2}. \tag{26}$$

Now, we are in the position to examine the dynamics of the entanglement and quantum correlations between the two bosonic modes. These modes are characterized by the covariance matrix outlined in Eq. (25). Throughout this investigation, we utilize two distinct measures: GQD ($\mathcal{D}_{\mathcal{G}}$) and GLN ($\mathcal{N}$) in Gaussian states. The numerical findings, are illustrated in the following figures. The reported results are obtained by varying the different parameters characterizing the initial state as well as the environment. Furthermore, to shed light on how quantum correlations evolve during environmental interactions, we have graphically represented the temporal changes in both GQD and GLN in Gaussian contexts.



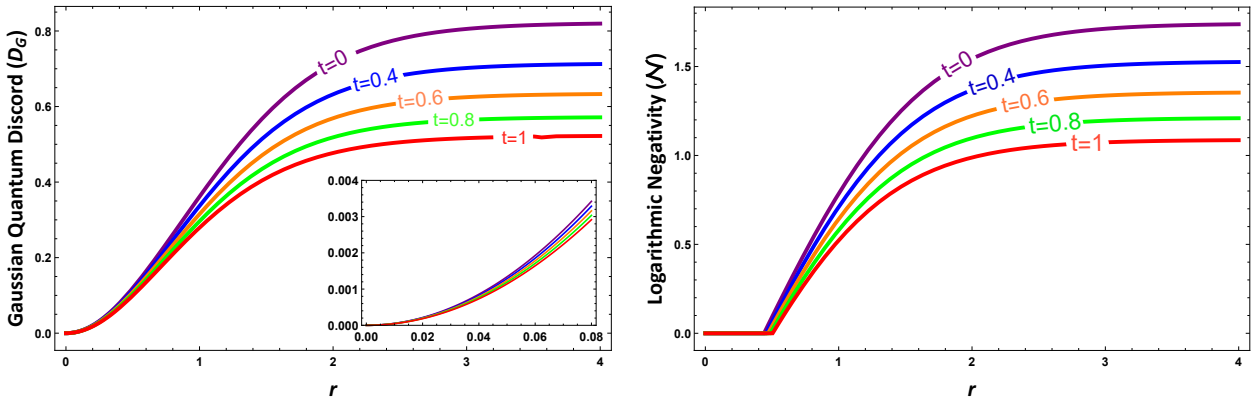
(a) (b)

FIGURE 2: The graphical representation of GQD ($\mathcal{D}_\mathcal{G}$) and GLN ($\mathcal{N}$) for bipartite Gaussian states is shown as a function of the rotation angle θ. Fig. (2a) presents the variation of GQD with θ for different time intervals t, with mean photon numbers $\bar{n}_1 = \bar{n}_2 = 0.5$ and an initial squeezing parameter $r = 0.5$. Fig. (2b) shows the behavior of GLN with θ for different values of t, under the same environmental conditions but with $r = 1.25$. A larger squeezing parameter is required because GLN cannot detect quantum correlations for small r values, as discussed in Fig. (3). The damping rate is fixed at $\Gamma = 1$.

The observed periodic behavior of quantum correlations with respect to the rotation angle θ originates from the interference mechanism induced by the phase-space rotation operation. Since the rotation operator behaves similarly to a beam splitter transformation, the redistribution of quantum fluctuations between the two modes becomes strongly dependent on the relative phase angle. The maxima observed around $\theta = \pi(1+k)/2$ correspond to configurations where the interference between the modes maximizes the transfer of quantum correlations. On the other hand, the progressive reduction of both $\mathcal{D}_\mathcal{G}$ and $\mathcal{N}$ with increasing interaction time reflects the detrimental influence of environmental decoherence. As the system interacts with the thermal Gaussian bath, incoherent noise and dissipation gradually suppress the non-classical correlations initially generated by the squeezing operation.

Fig. (2) presents the evolution of GQD ($\mathcal{D}_\mathcal{G}$) and GLN ($\mathcal{N}$) in Gaussian States as a function of the initial rotation angle θ, across different time intervals t of interaction with the Gaussian environment. The data illustrated in this figure reveals that the peak values for both $\mathcal{D}_\mathcal{G}$ and $\mathcal{N}$ occur at $\theta = \frac{\pi}{2}(1+k)$, with $k \in \mathbb{Z}$, particularly at short periods of interaction times t. Furthermore, the patterns of both measures show a similar, periodic nature with a period of $\theta = \pi/2$. This pattern suggests that the output state encompasses a higher amont of quantum correlation, notably at lower t values and when θ aligns with $\frac{\pi}{2}(1+k)$. It's also observed that prolonged interaction periods with the Gaussian environment generally diminish the system's quantum correlations. The results for $\mathcal{D}_\mathcal{G}$ are specifically based on an initial squeezing parameter of $r = 0.5$, while those for $\mathcal{N}$ are derived from an initial

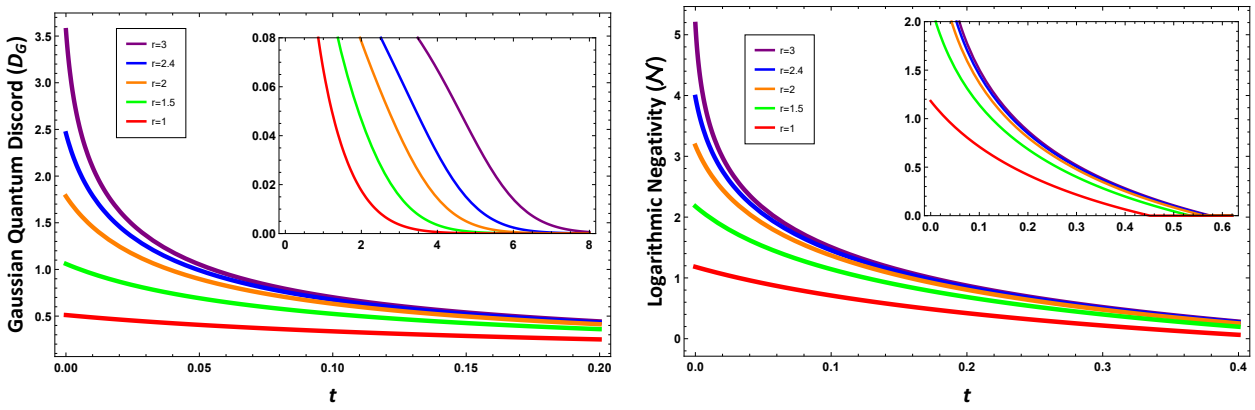
squeezing parameter of $r = 1.25$. To explore the reasons behind these differences, we compare in Fig. (3) the behaviors of $\mathcal{D}_\mathcal{G}$ and $\mathcal{N}$ versus the initial squeezing parameter r.



(a) (b)

FIGURE 3: The figure illustrates the behavior of GQD ($\mathcal{D}_\mathcal{G}$) and GLN ($\mathcal{N}$) of the bipartite Gaussian output state as functions of the initial squeezing parameter r. Figure (3a) shows the evolution of $\mathcal{D}_\mathcal{G}$ with r for different times t, while Fig. (3b) presents the corresponding variation of $\mathcal{N}$. In both cases, the parameters are fixed at $\bar{n}_1 = \bar{n}_2 = 0.5$, initial rotation angle $\pi/2$, and damping rate $\Gamma = 1$.

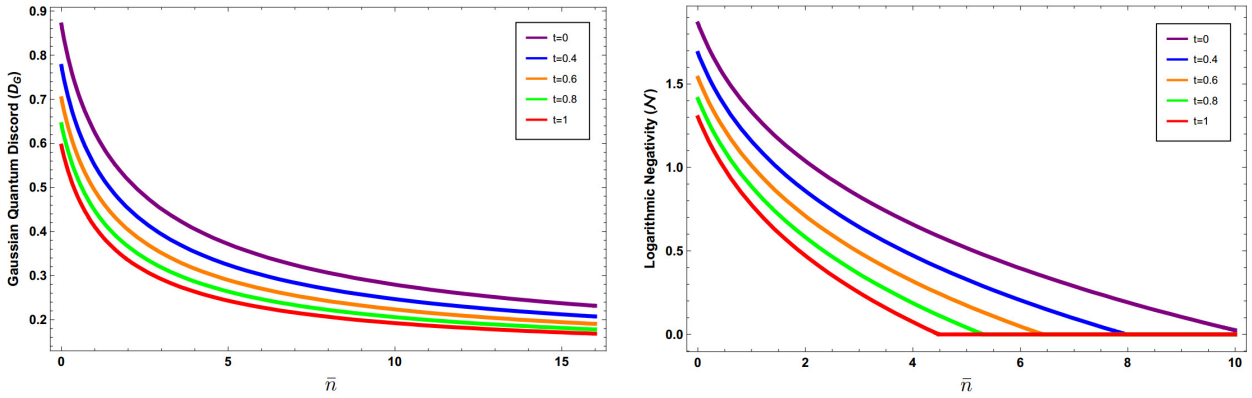
We shall examine how quantum correlations, as quantified by $\mathcal{D}_\mathcal{G}$ and $\mathcal{N}$, respond to adjustments in the initial squeezing parameter r over various time intervals t. As illustrated in Fig. (3a) and Fig. (3b), both $\mathcal{D}_\mathcal{G}$ and $\mathcal{N}$ demonstrate similar responses to changes in r across different t durations. we notice, from Figs. 3a and 3b that for lower values of the squeezing parameter, quantum discord is more appropriate than GLN in capturing quantum correlations. Specifically, for r values ranging from 0 to 1, $\mathcal{N}$ suggests vanishing of quantum correlations, even though the two modes exhibit correlation for any non-zero squeezing parameter, and as r takes higher values, we attain a maximally entangled state. This discrepancy hints at the relative insensitivity of $\mathcal{N}$ in comparison to $\mathcal{D}_\mathcal{G}$ in capturing quantum correlations. The distinction between the capabilities of $\mathcal{D}_\mathcal{G}$ and $\mathcal{N}$ in recognizing quantum correlations will be further explored in the subsequent figure (Fig. (4)), where we plot the evolution of $\mathcal{D}_\mathcal{G}$ and $\mathcal{N}$ as a function of the interaction time.



(a) (b)

FIGURE 4: The figure shows the time evolution of GQD ($\mathcal{D}_{\mathcal{G}}$) and GLN ($\mathcal{N}$) for bipartite Gaussian states interacting with a Gaussian environment. Fig. (4a) presents the dynamics of $\mathcal{D}_{\mathcal{G}}$ for different squeezing parameters r, with $\bar{n}_1 = \bar{n}_2 = 0.5$ and $\theta = \pi/2$. Fig. (4b) displays the corresponding evolution of $\mathcal{N}$ under the same conditions. The damping rate is fixed at $\Gamma = 1$.

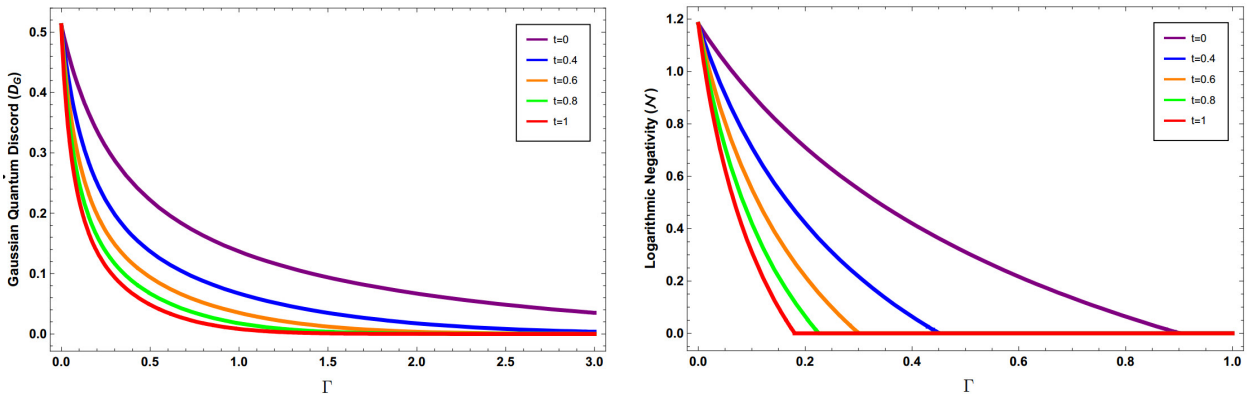
In Fig. (4), we illustrate the temporal dynamics of GQD ($\mathcal{D}_{\mathcal{G}}$) and GLN ($\mathcal{N}$) in Gaussian States as a function of time t. The results presented in Fig. (4a) and Fig. (4b) reveal that, as the interaction time t becomes large, both $\mathcal{D}_{\mathcal{G}}$ and $\mathcal{N}$ serve as indicators of the quantum correlations existing between the two output modes. This observation mainly stems from the limited influence of the Gaussian environment over shorter interaction periods. However, as the duration of environmental interaction is prolonged, the correlation levels identified by $\mathcal{N}$ diminish towards zero, reflecting the significant impact of the Gaussian environmental conditions. Moreover, the temporal evolution of $\mathcal{D}_{\mathcal{G}}$ shows its resilience facing the of environmental effects, maintaining its capability to indicate quantum correlations despite extended exposure to the Gaussian environment.



(a) (b)

FIGURE 5: Gaussian Quantum Discord (GQD), $\mathcal{D}_G$, and Gaussian Logarithmic Negativity (GLN), $\mathcal{N}$, of the bipartite Gaussian output state as functions of the mean photon number $\bar{n}$ for different values of time t. (a) The GQD decreases monotonically with increasing $\bar{n}$, with lower values obtained for larger t. (b) The GLN also decreases with increasing $\bar{n}$ and vanishes at a finite value of $\bar{n}$, which shifts toward smaller $\bar{n}$ as t increases. The parameters are fixed at $r = 2$, initial rotation angle $\pi/2$, and damping rate $\Gamma = 1$.

Figure 5 examines the behavior of the Gaussian Quantum Discord ($\mathcal{D}_\mathcal{G}$) and the Gaussian Logarithmic Negativity ($\mathcal{N}$) as functions of the mean photon number $\bar{n}$ for different values of the interaction time t, with the parameters fixed at $r = 2$, $\theta = \pi/2$, and $\Gamma = 1$. In Fig. 5a, the GQD decreases monotonically with increasing $\bar{n}$, reflecting the degradation of quantum correlations as the thermal noise of the environment intensifies. However, despite this monotonic decay, $\mathcal{D}_\mathcal{G}$ never vanishes completely; it approaches a nonzero asymptotic value even for large $\bar{n}$. This behavior is qualitatively consistent with the results of Fig. 4a, where GQD survived asymptotically in time. Moreover, increasing the interaction time t shifts the curves downward, indicating that longer exposure to the noisy environment reduces the amount of discord, yet the qualitative robustness of GQD persists. In contrast, Fig. 5b shows that the GLN $\mathcal{N}$ not only decreases with increasing $\bar{n}$ but also vanishes at a finite critical value $\bar{n}_{\text{crit}}$. This disappearance of entanglement—often referred to as entanglement sudden death—occurs earlier (i.e., at smaller $\bar{n}$) as the interaction time t increases. This finding is fully consistent with the sudden death of entanglement observed in Fig. 4b, where GLN vanished at a finite time. Furthermore, the behavior of GLN in Fig. 5b mirrors its response to the squeezing parameter r in Fig. 3b, where $\mathcal{N}$ remained zero for small r while GQD was already nonzero. Taken together, Fig. 5 confirms that the superiority of GQD over GLN in detecting quantum correlations is not limited to variations in r or t, but extends to the environmental parameter $\bar{n}$. The GQD captures correlations that persist even when entanglement is completely destroyed by thermal noise, whereas GLN is only sensitive to entanglement and thus vanishes at a finite threshold. This reinforces the central claim of the manuscript: GQD is a more resilient and more general quantifier of quantum correlations in Gaussian environments.



(a) (b)

FIGURE 6: Gaussian Quantum Discord (GQD), $\mathcal{D}_G$, and Gaussian Logarithmic Negativity (GLN), $\mathcal{N}$, as functions of the damping rate Γ for different values of time t. (a) The GQD decreases monotonically with Γ, while (b) the GLN decreases and vanishes at a finite value of Γ. In both cases, increasing t accelerates the decay of quantum correlations. The parameters are fixed at $r = 2$, initial rotation angle $\pi/2$, and $\bar{n} = 0.5$.

Figure 6 investigates the dynamics of GQD ($\mathcal{D}_\mathcal{G}$) and GLN ($\mathcal{N}$) as functions of the damping rate Γ for different values of the interaction time t, with the parameters fixed at $r = 2$, $\theta = \pi/2$, and $\bar{n} = 0.5$. In Fig. 6a, the GQD decreases monotonically with increasing Γ, reflecting the expected degradation of quantum correlations as the dissipative coupling to the environment strengthens. However, similar to the behavior observed in Fig. 5a, $\mathcal{D}_\mathcal{G}$ does not vanish completely; it approaches a nonzero asymptote even for large damping rates. This persistence of discord under strong damping is consistent with the asymptotic survival of GQD observed in Fig. 4a and reinforces the conclusion that GQD is robust against environmental decoherence. As the interaction time t increases, the curves shift downward, indicating that longer exposure to the damping environment reduces the amount of discord, yet the qualitative resilience of GQD remains intact. In contrast, Fig. 6b shows that the GLN $\mathcal{N}$ decreases with increasing Γ and vanishes at a finite critical damping rate Γ_{crit}. This disappearance of entanglement occurs earlier (i.e., at smaller Γ) as the interaction time t increases, mirroring the sudden death of entanglement observed in Fig. 4b and Fig. 5b. The behavior of GLN in Fig. 6b is also consistent with its response to the squeezing parameter r in Fig. 3b, where $\mathcal{N}$ remained zero for small r while GQD was already nonzero. The comparison between Fig. 6a and Fig. 6b clearly demonstrates that GQD is significantly more resilient than GLN against the damping rate Γ. While entanglement undergoes sudden death at a finite Γ_{crit}, quantum discord persists indefinitely, capturing non-classical correlations that survive even in the strong-damping regime. This finding provides further evidence that GQD is a more appropriate quantifier for characterizing quantum correlations in noisy Gaussian channels, as it reveals the presence of non-classical correlations beyond entanglement that are otherwise invisible to GLN. The results of Fig. 6, together with those of Figs. 3, 4, and 5, establish a consistent and unified picture: across all relevant parameters—squeezing r, time t, mean photon number $\bar{n}$, and damping

rate Γ—GQD consistently outperforms GLN in detecting and quantifying quantum correlations in Gaussian thermal environments.

5 Conclusion

Continuous-variable systems strongly rely on Gaussian states and Gaussian operations, mainly because the vacuum state of quantum electrodynamics is intrinsically Gaussian. This makes Gaussian states essential resources for quantum information processing and motivates the investigation of their non-classical correlations. In this work, we studied the dynamics of quantum correlations in two-mode Gaussian states interacting with a Gaussian thermal environment. These correlations were quantified using GQD ($\mathcal{D}_{\mathcal{G}}$) and GLN ($\mathcal{N}$). Their evolution was analyzed through the covariance matrix formalism as a function of the interaction time and environmental parameters. Our results show that GQD is significantly more robust against environmental decoherence than GLN , revealing the persistence of non-classical correlations even after the disappearance of entanglement. From a physical perspective, the present model provides a realistic description of continuous-variable quantum systems propagating in noisy optical environments. Therefore, these findings may contribute to a better understanding of the robustness of Gaussian quantum correlations in practical applications such as quantum communication, optical fibers, and continuous-variable quantum sensing technologies operating under realistic noisy conditions.

The data availability statement

The authors declare that they have no known competing financial interests or personal relationships that could have appeared to influence the work reported in this paper.

References

[1] C. Weedbrook, S. Pirandola, R. García-Patrón, N. J. Cerf, T. C. Ralph, J. H. Shapiro, and S. Lloyd, "Gaussian quantum information," *Rev. Mod. Phys.* **84**, 621–669 (2012).

[2] M. M. Wilde, *Quantum Information Theory*, Cambridge University Press, Cambridge (2013).

[3] N. Gisin and R. Thew, "Quantum communication," *Nat. Photonics* **1**, 165–171 (2007).

[4] G.-L. Long, F.-G. Deng, C. Wang, X.-H. Li, X.-R. Wen, and X. Zhang, "Quantum secure direct communication and deterministic secure quantum communication," *Front. Phys. China* **2**, 251–272 (2007).

[5] A. Pathak, *Elements of Quantum Computation and Quantum Communication*, CRC Press, Boca Raton (2013).

[6] H. M. Wiseman and G. J. Milburn, *Quantum Measurement and Control*, Cambridge University Press, Cambridge (2009).

[7] V. B. Braginsky, F. Ya. Khalili, and K. S. Thorne, *Quantum Measurement*, Cambridge University Press, Cambridge (1992).

[8] Y. Lahlou, B. Maroufi, and M. Daoud, "Investigating entangled photons to quantify quantum correlations in dual optomechanical cavities," *Chin. J. Phys.* **89**, 16–26 (2024).

[9] T. D. Ladd, F. Jelezko, R. Laflamme, Y. Nakamura, C. Monroe, and J. L. O'Brien, "Quantum computers," *Nature* **464**, 45–53 (2010).

[10] A. Steane, "Quantum computing," *Rep. Prog. Phys.* **61**, 117–173 (1998).

[11] M. A. Nielsen and I. L. Chuang, *Quantum Computation and Quantum Information*, Cambridge University Press, Cambridge (2000).

[12] R. de Vivie-Riedle and U. Troppmann, "Femtosecond lasers for quantum information technology," *Chem. Rev.* **107**, 5082–5100 (2007).

[13] U. L. Andersen, G. Leuchs, and C. Silberhorn, "Continuous-variable quantum information processing," *Laser Photonics Rev.* **4**, 337–354 (2010).

[14] Y. Lahlou, M. Amazioug, J. El Qars, N. Habiballah, M. Daoud, and M. Nassik, "Quantum coherence versus non-classical correlations in optomechanics," *Int. J. Mod. Phys. B* **33**, 1950343 (2019).

[15] B. Yurke, "Squeezed-coherent-state generation via four-wave mixers and detection via homodyne detectors," *Phys. Rev. A* **32**, 300–310 (1985).

[16] R. F. Werner and M. M. Wolf, "Bound entangled Gaussian states," *Phys. Rev. Lett.* **86**, 3658–3661 (2001).

[17] J. DiGuglielmo, A. Samblowski, B. Hage, C. Pineda, J. Eisert, and R. Schnabel, "Experimental unconditional preparation and detection of a continuous bound entangled state of light," *Phys. Rev. Lett.* **107**, 240503 (2011).

[18] S. L. Braunstein and P. van Loock, "Quantum information with continuous variables," *Rev. Mod. Phys.* **77**, 513–577 (2005).

[19] B. L. Schumaker, "Quantum mechanical pure states with Gaussian wave functions," *Phys. Rep.* **135**, 317–408 (1986).

[20] S. Olivares, "Quantum optics in the phase space: A tutorial on Gaussian states," *Eur. Phys. J. Spec. Top.* **203**, 3–24 (2012).

[21] M. M. Wolf, D. Pérez-García, and G. Giedke, "Quantum capacities of bosonic channels," *Phys. Rev. Lett.* **98**, 130501 (2007).

[22] R. Bellman, "A Markovian decision process," *J. Math. Mech.* **6**, 679–684 (1957).

[23] S. Olivares, M. G. A. Paris, and A. R. Rossi, "Optimized teleportation in Gaussian noisy channels," *Phys. Lett. A* **319**, 32–43 (2003).

[24] L. Bakmou and M. Daoud, "Ultimate precision of joint parameter estimation under noisy Gaussian environment," *Phys. Lett. A* **428**, 127947 (2022).

[25] L. Banchi, S. L. Braunstein, and S. Pirandola, "Quantum fidelity for arbitrary Gaussian states," *Phys. Rev. Lett.* **115**, 260501 (2015).

[26] T. C. Ralph, "Quantum error correction of continuous-variable states against Gaussian noise," *Phys. Rev. A* **84**, 022339 (2011).

[27] H. Nha and H. J. Carmichael, "Proposed test of quantum nonlocality for continuous variables," *Phys. Rev. Lett.* **93**, 020401 (2004).

[28] H. M. Wiseman, S. J. Jones, and A. C. Doherty, "Steering, entanglement, nonlocality, and the Einstein-Podolsky-Rosen paradox," *Phys. Rev. Lett.* **98**, 140402 (2007).

[29] Y. Lahlou, B. Maroufi, and M. Daoud, "Quantum correlations and entanglement in coupled optomechanical resonators with photon hopping via Gaussian interferometric power analysis," *Chin. Phys. B* **33**, 050303 (2024).

[30] I. Bengtsson and K. Życzkowski, *Geometry of Quantum States: An Introduction to Quantum Entanglement*, Cambridge University Press, Cambridge (2017).

[31] R. Horodecki, P. Horodecki, M. Horodecki, and K. Horodecki, "Quantum entanglement," *Rev. Mod. Phys.* **81**, 865–942 (2009).

[32] Y. Lahlou, B. Maroufi, and M. Daoud, "Quantifying quantum correlations beyond entanglement via robust photon hopping in an optomechanical system," *Mod. Phys. Lett. A* **38**, 2350154 (2023).

[33] G. Adesso, *Entanglement of Gaussian States*, Ph.D. thesis, University of Salerno, Italy (2007).

[34] E. Wu, J. Liu, L.-M. Chao, J. Qiao, J.-Y. Niu, J.-L. He, Y. Zhang, and Y.-H. Ma, "Generation of quadripartite continuous-variable entanglement in two coupled opto-mechanical systems," *Laser Phys.* **30**, 065205 (2020).

[35] A. P. Lund, T. C. Ralph, and H. L. Haselgrove, "Fault-tolerant linear optical quantum computing with small-amplitude coherent states," *Phys. Rev. Lett.* **100**, 030503 (2008).

[36] D. Beaver and S. Haber, "Cryptographic protocols provably secure against dynamic adversaries," in *Advances in Cryptology – CRYPTO '92*, Lecture Notes in Computer Science, Vol. 740, Springer, Berlin (1993).

[37] S. Pirandola, J. Eisert, C. Weedbrook, A. Furusawa, and S. L. Braunstein, "Advances in quantum teleportation," *Nat. Photonics* **9**, 641–652 (2015).

[38] V. Giovannetti, S. Lloyd, and L. Maccone, "Quantum metrology," *Phys. Rev. Lett.* **96**, 010401 (2006).

[39] R. Nichols, P. Liuzzo-Scorpo, P. A. Knott, and G. Adesso, "Multiparameter Gaussian quantum metrology," *Phys. Rev. A* **98**, 012114 (2018).

[40] L. Bakmou, M. Daoud, and R. Ahl Laamara, "Multiparameter quantum estimation theory in quantum Gaussian states," *J. Phys. A: Math. Theor.* **53**, 385301 (2020).

[41] C. F. Li, Y. S. Zhang, Y. F. Huang, and G. C. Guo, "Quantum strategies of quantum measurements," *Phys. Lett. A* **280**, 257–260 (2001).

[42] M. I. Kolobov and C. Fabre, "Quantum limits on optical resolution," *Phys. Rev. Lett.* **85**, 3789–3792 (2000).

[43] A. J. Den Dekker and A. van den Bos, "Resolution: A survey," *J. Opt. Soc. Am. A* **3**, 547–557 (1986).

[44] Y. Lahlou, B. Maroufi, J. El Qars, and M. Daoud, "Gaussian intrinsic entanglement and more general quantum correlations of two mechanical oscillators," *J. Russ. Laser Res.* **41**, 584–596 (2020).

[45] P. R. Berman and V. S. Malinovsky, *Principles of Laser Spectroscopy and Quantum Optics*, Princeton University Press, Princeton (2011).

[46] Y. Subaşı, L. Cincio, and P. J. Coles, "Entanglement spectroscopy with a depth-two quantum circuit," *J. Phys. A: Math. Theor.* **52**, 044001 (2019).

[47] D. Girolami, T. Tufarelli, and G. Adesso, "Quantum discord determines the interferometric power of quantum states," *Phys. Rev. Lett.* **112**, 210401 (2014).

[48] D. T. Smithey, M. Beck, M. G. Raymer, and A. Faridani, "Measurement of the Wigner distribution and the density matrix of a light mode using optical homodyne tomography: Application to squeezed states and the vacuum," *Phys. Rev. Lett.* **70**, 1244–1247 (1993).

[49] M. F. Sacchi, "Optimal discrimination of quantum operations," *Phys. Rev. A* **71**, 062340 (2005).

[50] D. Zhou and R. Joynt, "Phenomenological noise model for superconducting qubits: Two-state fluctuators and $1/f$ noise," *Supercond. Sci. Technol.* **25**, 045003 (2012).

[51] Y. Lahlou, L. Bakmou, B. Maroufi, and M. Daoud, "Quantifying quantum correlations in noisy Gaussian channels," *Quantum Inf. Process.* **21**, 248 (2022).

[52] G. M. Zaslavsky, "Stochasticity in quantum systems," *Phys. Rep.* **80**, 157–250 (1981).

[53] C. Benedetti, F. Buscemi, P. Bordone, and M. G. A. Paris, "Dynamics of quantum correlations in colored-noise environments," *Phys. Rev. A* **87**, 052328 (2013).

[54] J. Maziero, T. Werlang, F. F. Fanchini, L. C. Céleri, and R. M. Serra, "System-reservoir dynamics of quantum and classical correlations," *Phys. Rev. A* **81**, 022116 (2010).

[55] C. Wang and Q.-H. Chen, "Exact dynamics of quantum correlations of two qubits coupled to bosonic baths," *New J. Phys.* **15**, 103020 (2013).

[56] W. H. Zurek, "Decoherence, einselection, and the quantum origins of the classical," *Rev. Mod. Phys.* **75**, 715–775 (2003).

[57] J. Maziero, L. C. Céleri, R. M. Serra, and V. Vedral, "Classical and quantum correlations under decoherence," *Phys. Rev. A* **80**, 044102 (2009).

[58] M. O. Scully and M. S. Zubairy, *Quantum Optics*, Cambridge University Press, Cambridge (1997).

[59] P. M. Chaikin and T. C. Lubensky, *Principles of Condensed Matter Physics*, Cambridge University Press, Cambridge (1995).

[60] K. Vogel and H. Risken, "Determination of quasiprobability distributions in terms of probability distributions for the rotated quadrature phase," *Phys. Rev. A* **40**, 2847–2849 (1989).

[61] V. I. Tatarskii, "The Wigner representation of quantum mechanics," *Sov. Phys. Usp.* **26**, 311–327 (1983).

[62] R. Simon, E. C. G. Sudarshan, and N. Mukunda, "Gaussian-Wigner distributions in quantum mechanics and optics," *Phys. Rev. A* **36**, 3868–3880 (1987).

[63] A. Ferraro, S. Olivares, and M. G. A. Paris, *Gaussian States in Continuous Variable Quantum Information*, arXiv:quant-ph/0503237 (2005).

[64] G. Adesso and A. Datta, "Quantum versus classical correlations and global purity in Gaussian states," *Phys. Rev. Lett.* **105**, 030501 (2010).

[65] G. Vidal and R. F. Werner, "Computable measure of entanglement," *Phys. Rev. A* **65**, 032314 (2002).

[66] A. Serafini, F. Illuminati, and S. De Siena, "Symplectic invariants, entropic measures and correlations of Gaussian states," *J. Phys. B: At. Mol. Opt. Phys.* **37**, L21–L28 (2004).

[67] K. Audenaert, M. B. Plenio, and J. Eisert, "Entanglement cost under positive-partial-transpose-preserving operations," *Phys. Rev. Lett.* **90**, 027901 (2003).

[68] M. B. Plenio, "Logarithmic negativity: A full entanglement monotone that is not convex," *Phys. Rev. Lett.* **95**, 090503 (2005).

[69] J. Eisert, *Entanglement in Quantum Information Theory*, Ph.D. thesis, University of Potsdam, Potsdam (2001).

[70] M. B. Plenio, "Logarithmic negativity: A full entanglement monotone that is not convex," arXiv:quant-ph/0505071 (2005).

[71] G. Adesso, A. Serafini, and F. Illuminati, "Extremal entanglement and mixedness in continuous variable systems," *Phys. Rev. A* **70**, 022318 (2004).

[72] S. L. Braunstein and C. M. Caves, "Statistical distance and the geometry of quantum states," *Phys. Rev. Lett.* **72**, 3439–3443 (1994).

[73] M. G. A. Paris, "Quantum estimation for quantum technology," *Int. J. Quantum Inf.* **7**, 125–137 (2009).

[74] K. Życzkowski and H.-J. Sommers, "Average fidelity between random quantum states," *Phys. Rev. A* **71**, 032313 (2005).

[75] M. Hayashi and K. Matsumoto, "Asymptotic performance of optimal state estimation in qubit system," *J. Math. Phys.* **49**, 102101 (2008).

[76] J. Kahn and M. Guta, "Local asymptotic normality for finite dimensional quantum systems," *Commun. Math. Phys.* **289**, 597–652 (2009).

[77] A. Uhlmann, "Optimizing entropy relative to a channel or a subalgebra," arXiv:quant-ph/9701014 (1997).

[78] G. Adesso, "Gaussian interferometric power," *Phys. Rev. A* **90**, 022321 (2014).

[79] R. Laurenza, S. Tserkis, L. Banchi, S. L. Braunstein, T. C. Ralph, and S. Pirandola, "Tight bounds for private communication over bosonic Gaussian channels based on teleportation simulation with optimal finite resources," *Phys. Rev. A* **100**, 042301 (2019).

[80] C. H. Bennett, D. P. DiVincenzo, J. A. Smolin, and W. K. Wootters, "Mixed-state entanglement and quantum error correction," *Phys. Rev. A* **54**, 3824–3851 (1996).

[81] F. Verstraete, K. Audenaert, and B. De Moor, "Maximally entangled mixed states of two qubits," *Phys. Rev. A* **64**, 012316 (2001).

[82] B. M. Terhal and P. Horodecki, "Schmidt number for density matrices," *Phys. Rev. A* **61**, 040301(R) (2000).

[83] G. Giedke, M. M. Wolf, O. Krüger, R. F. Werner, and J. I. Cirac, "Entanglement of formation for symmetric Gaussian states," *Phys. Rev. Lett.* **91**, 107901 (2003).

[84] N. Takei, T. Aoki, S. Koike, K.-i. Yoshino, K. Wakui, H. Yonezawa, T. Hiraoka, J. Mizuno, M. Takeoka, M. Ban, and A. Furusawa, "Experimental demonstration of quantum teleportation of a squeezed state," *Phys. Rev. A* **72**, 042304 (2005).

[85] M. M. Wolf, G. Giedke, O. Krüger, R. F. Werner, and J. I. Cirac, "Gaussian entanglement of formation," *Phys. Rev. A* **69**, 052320 (2004).